Self Resonance Cancellation for Joint Torque Control Using Torque Sensor

Akiyuki Hasegawa* Student Member, Hiroshi Fujimoto* Senior Member
Taro Takahashi** Member

Demand for industrial robots in collaboration with people and nursing robots is increasing. In order to realize safe contact between robots and people, force control is required. We previously proposed Self Resonance Cancellation (SRC), position control method for two-inertial system. In this paper, we applied SRC to joint torque control by using torque sensor. Conventional SRC use motor-side and load-side encoders. Proposed SRC use torque sensor on shaft between motor-side and load-side. Proposed controller can be designed without plant parameters. The relationship between the two control parameters and the control performance is clear. Simulation and experimental results show the effectiveness of the proposed method.

Keywords: two-inertial system, vibration suppression control, torque sensor, self resonance cancellation, humanoid robot, joint torque

1. Introduction

Along with the development of robotics engineering, industrial robots that collaborate with human beings are required [2], in the welfare field, nursing care robots are being put into practical use [3]. Robots that work in coexistence with such people are required to control forces so as not to harm people. In this paper, torque transmitted by the transmission mechanism from the drive motor to the load side is called joint torque.

A joint of a humanoid robot using an electric motor is not directly connected to a load by a motor, but is connected to a load via a timing belt or a gear. The belt drive improves the degree of freedom of the motor arrangement and the gear makes it possible to obtain a large output torque with a small motor. Although both are general mechanisms, the rigidity of belts and gears is low. In order to improve the control performance of the entire leg, it is necessary to control a single joint in a high frequency region. However, an elastic body such as a belt and a gear in a joint causes resonance vibration and restricts the control band, therefore resonance suppression has become a subject of robot joint control.

In order to control the joint torque, it is necessary to estimate the joint torque with a reaction force observer or measure it with a torque sensor. In the past, since the rigidity of the torque sensor itself and the sensor band were low and it was difficult to use it for feedback control, study using a reaction force observer has been conducted. In the case of using the reaction force observer, since the estimated external force includes disturbance such as friction, much study on friction compensation has been done [4].

However, in recent years, sensors with high rigidity and high resolution have been developed, making it possible to use sensor values for feedback control, [5] [6]. In the future, it is expected that the number of devices having sensors for force control will increase.

In this paper, we design the proposed method based on Self Resonance Cancellation control (SRC) [1] which has been studied as a position control of two-inertial systems in this laboratory. SRC has the advantage of simplifying the design of the control parameters and is compatible with the advantage of the torque sensor which enables simple joint torque feedback. Combining SRC and torque sensor makes it possible to design a simple joint torque control system leaving the advantages of mutual simplicity, and designed a highly practical control system in industry. The proposed method for joint torque control makes it possible to intuitively adjust the control performance by tuning two parameters.

2. Experiment setup

A single joint of a robot can be modeled as a low dimensional model into two-inertial systems. Therefore, a two-inertial motor bench was used as an experimental machine for basic experiments. The Measured frequency characteristics of the two-inertial motor bench are shown in Fig.2.

Measurement of frequency characteristics was carried out with a method using multi-sine wave [7]. The parameter obtained by fitting the model from the measurement result is shown in Tab. 1.

3. Proposed Joint torque control by self resonance cancellation control using torque sensor

Demand for joint torque control in domestic robots and industrial robots is increasing so that joint torque control en-

* The University of Tokyo
5-1-5, Kashiwanoha, Kashiwa, Chiba, 227-8561 Japan
Phone: +81-4-7136-3881
Email: hasegawa16@hflab.k.u-tokyo.ac.jp
** Advanced Technology Engineering Department,Partner Robot Division, Toyota Motor Corporation
1-4-18, Koraku, Bunkyo-ku, Tokyo 112-8701, Japan
Email: taro_takahashi@mail.toyota.co.jp

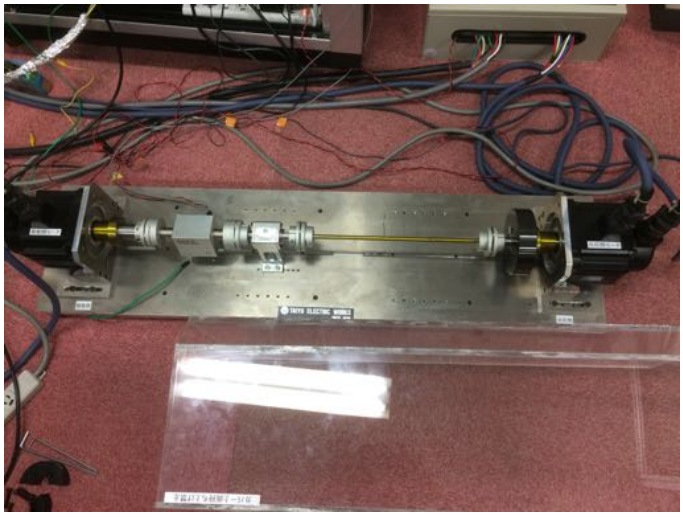

Fig. 1. Photo of two-inertial system motor bench

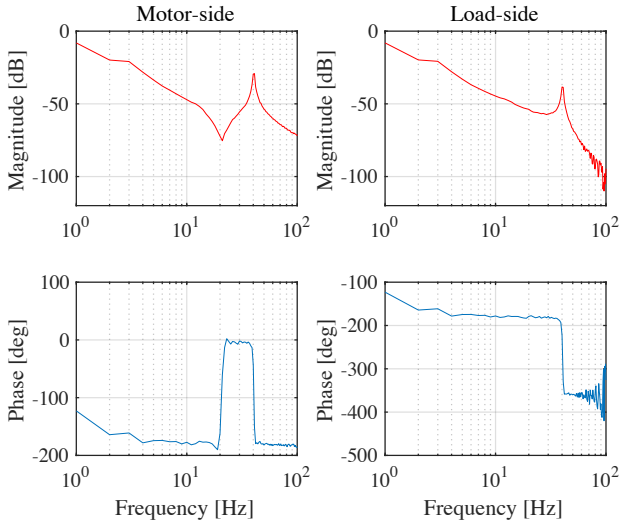

Fig. 2. Measured frequency characteristic of motor bench

Table 1. Fitting parameters of two-inertial motor benches

J_M	Motor-side moment of inertia	0.0019	kgm^2
D_M	Motor-side viscosity friction coefficient	0.0018	Nms/rad
K	Torsional rigidity coefficient	93.6137	N/m
J_L	Load-side moment of inertia	0.0057	kgm^2
D_L	Load-side viscosity friction coefficient	0.0826	Nms/rad

ables advanced work and safe collaboration work with humans. In consideration of such background, in this chapter, we propose joint torque control with reference to Frequency Separation Self-Resonant Cancellation Control (FS-SRC) [8] which is one of the two-inertial position control methods using SRC Propose a system.

3.1 Principle of Self Resonance Cancellation (SRC) [1]

In order to explain FS-SRC, the principle of SRC will be described first. Block diagram of SRC is shown in Fig.3. SRC calculates virtual angle θ_{SRC} from driving side angle and load side angle. θ_{SRC} is denoted by (1), and θ_{SRC} is the center of gravity of the driving side angle and the load side angle. θ_{SRC}

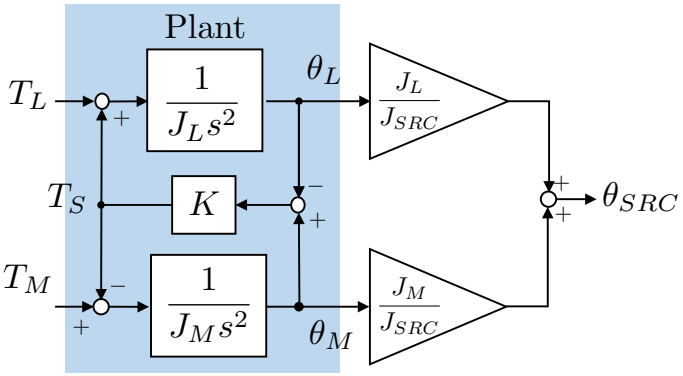

Fig. 3. Block diagram of SRC [1]

has no resonance, therefore feedback of θ_{SRC} makes higher control frequency.

$$\theta_{SRC} = \frac{J_M\theta_M}{J_M + J_L} + \frac{J_L\theta_L}{J_M + J_L}. \cdots\cdots (1)$$

$\ddot{\theta}_{SRC}$ is denoted by (4), because the equation of motion on the driving side and the load side in the inertial system is denoted by (2), (3) .

$$J_M\ddot{\theta}_M = T_M - K(\theta_M - \theta_L), \cdots\cdots (2)$$
$$J_L\ddot{\theta}_L = K(\theta_M - \theta_L), \cdots\cdots (3)$$
$$\ddot{\theta}_{SRC} = \frac{J_M\ddot{\theta}_M}{J_M + J_L} + \frac{J_L\ddot{\theta}_L}{J_L + J_L} = \frac{T_M}{J_M + J_L}. \cdots\cdots (4)$$

The transfer function from input torque T_M to θ_{SRC} is shown in (5). Since it is a rigid body model without resonance, the design of the controller becomes very simple.

$$\frac{\theta_{SRC}}{T_M} = \frac{1}{(J_M + J_L)s^2} = \frac{1}{J_{SRC}s^2}. \cdots\cdots (5)$$

However, even if θ_{SRC} is controlled, the load side angle deviates from the command value. Also, since θ_{SRC} neglects the resonance component, there is a problem that vibration suppression performance can not be improved.

3.2 Principle of Frequency Separation SRC (FS-SRC) [8]

FS-SRC is a control method that made it possible to intuitively adjust the Nyquist diagram utilizing the fact that SRC can create virtual angle which has no resonance. The control system of FS-SRC is shown in Fig.5. The virtual angle $\tilde{\theta}_L$ is denoted in (6).

$$\tilde{\theta}_L = \frac{\omega_c}{s + \omega_c}\theta_L + \frac{s}{s + \omega_c}\theta_\alpha = \frac{\omega_c}{s + \omega_c}\theta_L + \frac{s}{s + \omega_c}\{\alpha\theta_L + (1 - \alpha)\theta_M\}. \cdots\cdots (6)$$

$\frac{\omega_c}{s + \omega_c}$ is a first order Low Pass FiIter(LPF), $\frac{s}{s + \omega_c}$ is a first order High Pass FiIter(HPF). ω_c is the cut-off frequency. (6) shows that $\tilde{\theta}_L$ is almost equal to θ_L in a sufficiently low

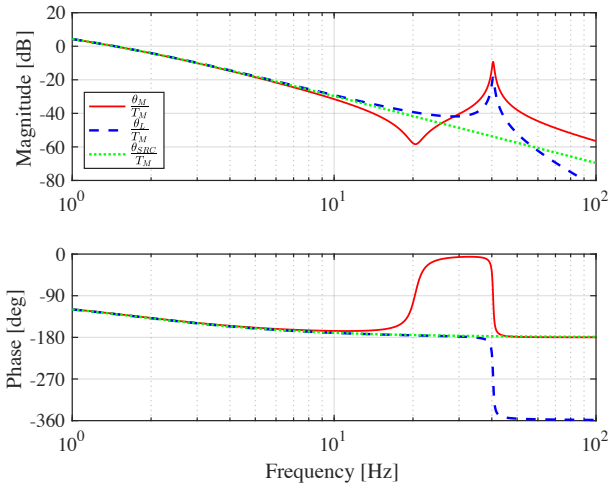

Fig. 4. Comparison of frequency characteristics of $\frac{\theta_M}{T_M}$ and $\frac{\theta_L}{T_M}$ and $\frac{\theta_{SRC}}{T_M}$

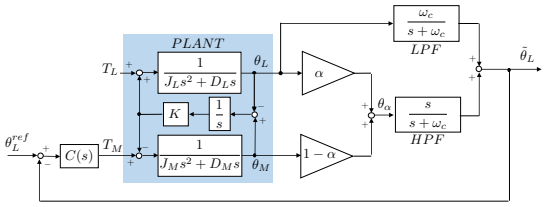

Fig. 5. Block Diagram of FS-SRC [8]

frequency region and almost equal to θ_α in a sufficiently high frequency region . When (7) is satisfied, the resonance component disappears from θ_α in the same way as SRC.

$$\alpha : (1-\alpha) = J_L : J_M \cdots\cdots\cdots\cdots\cdots\cdots\cdots\cdots (7)$$

Here, in FS-SRC, rather than completely eliminating the resonance component, adjust α to create a virtual angle θ_α with a little resonance component. Leaving a little resonance component makes it possible to have resonance suppression function by feedback of θ_α. After all, in the low frequency region without resonance, it is possible to control directly feedbacking θ_L, and in the high frequency region affected by the resonance, feedback θ_α with a little resonance component.

Therefore, since $\tilde{\theta}_L$ has no resonance component in the low frequency region and has only a small resonance component even in the high frequency region, just design the controller C(s) for the rigid body is sufficient. In other words, since the transfer function of the plant is $\dfrac{1}{J_{SRC}s^2 + D_{SRC}s}$, pole assignment is possible with PI controller.

Relations between parameters and Nyquist diagrams in FS-SRC are shown in Fig.6 and Fig.7.

In FS-SRC adjust the degree of resonance suppression with α and adjust phase compensation with ω_c. By adjusting α and cutoff frequency ω_c, we realize a sensitivity function that is balanced between resonance frequency and other frequencies.

3.3 Proposal of SRC using torque sensor(TSRC) FS-SRC was a method based on SRC. In designing joint torque FS-SRC(FS-TSRC), firstly, SRC using a torque sensor (TSRC) was designed. SRC adds the equations of motion on the motor-side and the load-side of two-inertial system, and cancels $T_S = K(\theta_M - \theta_L)$. (2) (3) shows that the motor-side value in the SRC is $\dfrac{T_M - T_S}{J_{SRC}s^2}$, lord-side value in the SRC is $\dfrac{T_S}{J_{SRC}s^2}$. Therefore, they can be obtained by measuring T_S using a torque sensor.

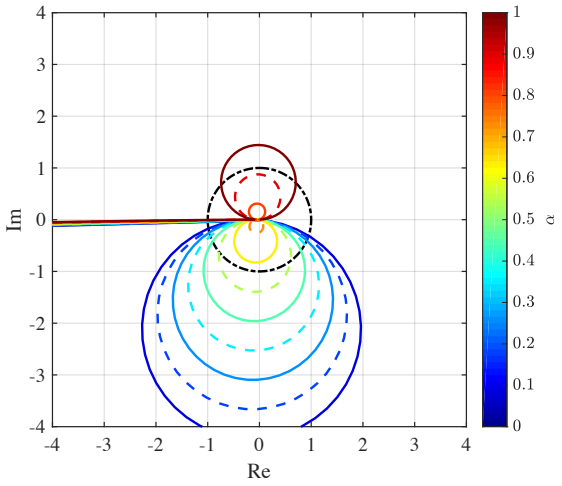

Fig. 6. Relations between parameters and Nyquist diagrams in FS-SRC $f_c = 0,\ \alpha : 0 \to 1$

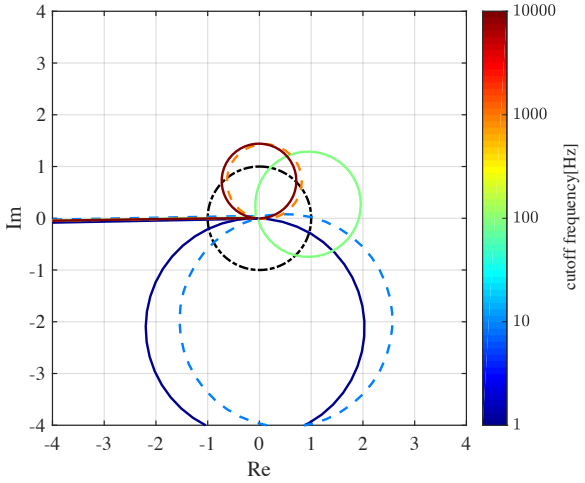

Fig. 7. Relations between parameters and Nyquist diagrams in FS-SRC $f_c : 0 \to \infty,\ \alpha : 0$

Fig.8 shows block diagram of TSRC. Regardless of the plant's parameters, TSRC will be rigidified if $T_M - T_S$ and T_S are added. However, when rigidification is made, the virtual torque T_{SRC} becomes the input valueT_M, therefore effective control can not be performed as it is.

3.4 Proposal of joint torque control FS-SRC (FS-TSRC) Torque dimension FS-SRC (FS-TSRC) was designed using torque sensor. The control system of FS-TSRC is shown in Fig.9.

The virtual torque $\tilde{T}_S$ is denoted in (8).

$$\tilde{T}_S = \frac{\omega_c}{s+\omega_c}T_S + \frac{s}{s+\omega_c}T_\alpha,$$

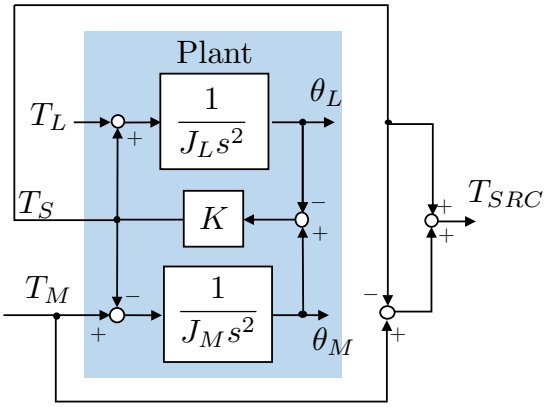

Fig. 8. Block Diagram of TSRC

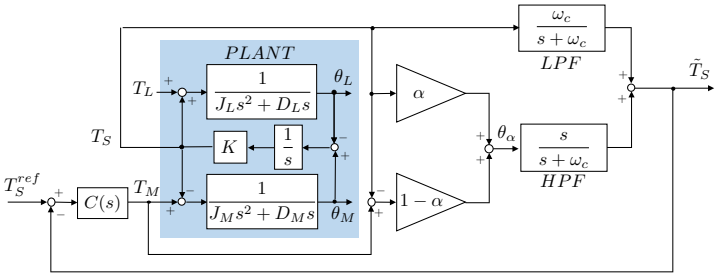

Fig. 9. Block Diagram of FS-TSRC

$$= \frac{\omega_c}{s+\omega_c} T_S + \frac{s}{s+\omega_c} \{\alpha T_S + (1-\alpha)(T_M - T_S)\},$$
$$= \frac{\omega_c}{s+\omega_c} T_S + \frac{s}{s+\omega_c} \{(2\alpha - 1) T_S + (1-\alpha) T_M\}. \quad (8)$$

(8) shows that $\tilde{T}_S$ is almost equal to T_S in a sufficiently low frequency region and almost equal to T_α in a sufficiently high frequency region .

According to the same principle as FS-SRC, in the low frequency region without resonance, it is possible to control directly feedbacking T_S, and in the high frequency region affected by the resonance, feedback T_α with a little resonance component.

Where T_α is rigidified when $\alpha = 0.5$. In other words, unlike FS-SRC, even if we do not know the moment of inertia on the driving side and the load side, we can adjust the parameters as a guide that $\alpha = 0.5$ is made rigid. Also, the controller C(s) can be designed for a rigid body like FS-SRC. That is, considering the case of $\alpha = 0.5$, you can design for the transfer function $\frac{T_\alpha}{T_M} = 0.5$, therefore just a single integrator is enough to eliminate steady-state deviation. Therefore, you can easily adjust the characteristics simply by adjusting two parameters, α and ω_c.

Relations between parameters and Nyquist diagrams in FS-TSRC are shown in Fig.10 and Fig.11.

4. Simulation

Frequency response of FS-TSRC was evaluated by simulation. Parameters in the simulation were performed in three cases shown in Tab. 2.When using a controller C(s), an integrator controller with a gain of 30 was used.

A comparison of Nyquist diagrams of $\frac{\tilde{T}_S}{T_M}$ without a controller is shown in Fig.12. As the cutoff frequency f_c rises,

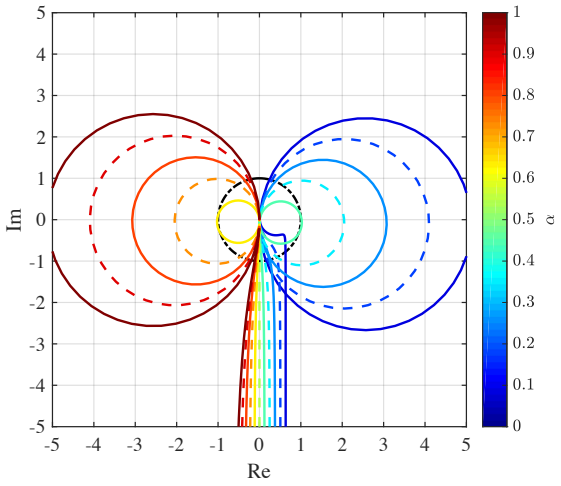

Fig. 10. Relations between parameters and Nyquist diagrams in FS-SRC $f_c = 0$Hz, $\alpha : 0 \rightarrow 1$

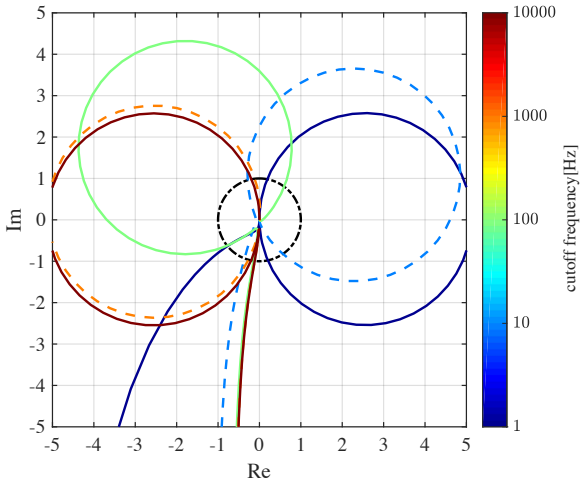

Fig. 11. Relations between parameters and Nyquist diagrams in FS-TSRC $f_c : 0 \rightarrow 10000$Hz, $\alpha : 0$

Table 2. Parameters of FS-TSRC

	α	f_{LPF}[Hz]
Case1	0.0	5
Case2	0.2	10
Case3	0.4	15

the phase advances, and as α approaches 0.5, the resonance component decreases and the rotation decreases.

A comparison of the frequency characteristics of the sensitivity function $\frac{T_S^{ref} - T_S}{T_S^{ref}}$ is shown in Fig.13. It can be seen that there is a tradeoff between disturbance suppression performance at low frequencies and disturbance suppression performance around resonance frequency.

A comparison of step responses of T_S is shown in Fig.14. It also shows that there is a tradeoff between disturbance suppression performance at low frequencies and disturbance suppression performance around resonance frequency.

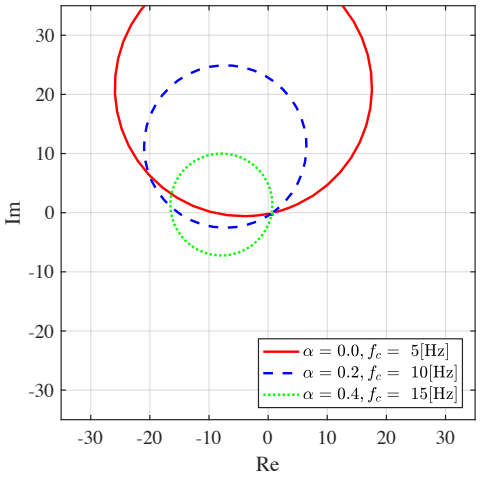

Fig. 12. Comparison of Nyquist diagrams of $\frac{\tilde{T}_S}{T_M}$ (Simulation)

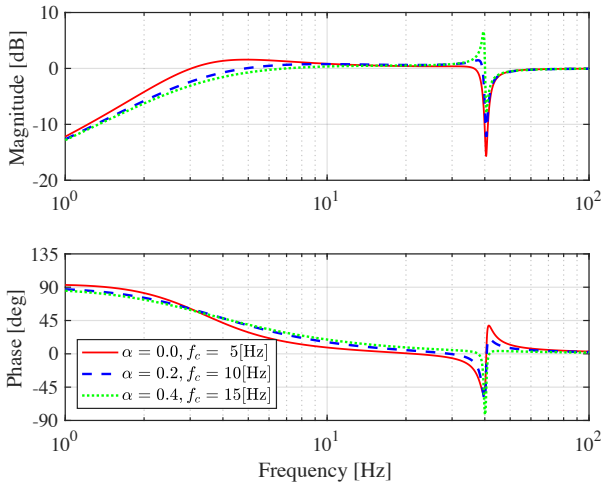

Fig. 13. Comparison of frequency characteristics of $\frac{T_S^{ref} - T_S}{T_S^{ref}}$ (Simulation)

5. Experiment

The frequency response of FS-TSRC was evaluated by experiment. Unipulse's torque sensor was used [6]. Parameters were performed in the three cases shown in Tab. 2 as in simulation. When using a controller C(s), an integrator controller with a gain of 30 was used.

A comparison of Nyquist diagrams of $\frac{\tilde{T}_S}{T_M}$ without a controller is shown in Fig.15. A comparison of the frequency characteristics of the sensitivity function $\frac{T_S^{ref} - T_S}{T_S^{ref}}$ is shown in Fig.16. A comparison of step responses of T_S is shown in Fig.17. Results very similar to simulation were obtained.

The reason why the peak of the sensitivity function is lowered in the experiment is considered to be the limit of frequency resolution and the existence of nonlinear friction that can not be modeled by identifying by frequency characteristic measurement.

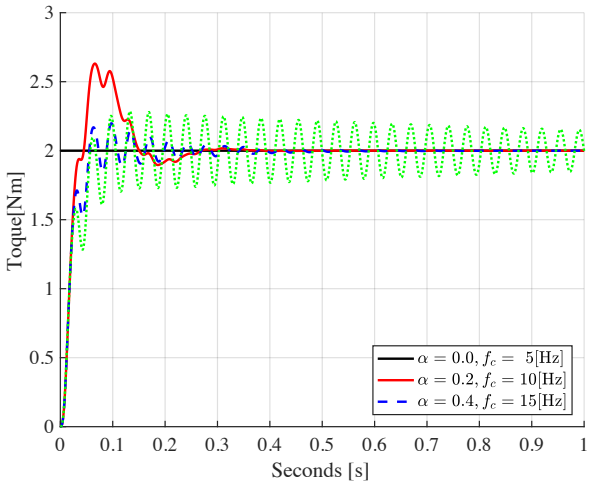

Fig. 14. Step response of T_S (Simulation)

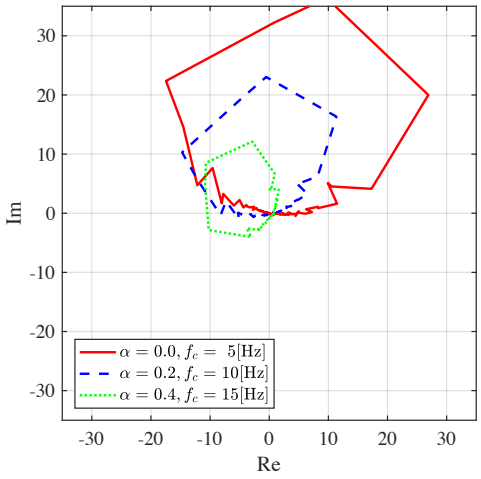

Fig. 15. Comparison of Nyquist diagrams of $\frac{\tilde{T}_S}{T_M}$ (Experiment)

It is considered that the vibration decreases with step response also due to the existence of nonlinear friction.

6. Conclusion

In the background that joint torque control enables sophisticated work and safe collaboration work with humans, the case of mounting torque sensors on domestic robots and industrial robots is increasing. In this paper, we proposed FS-TSRC, an joint torque control method using a torque sensor based on the position control method called FS-SRC. The performance of the controller of the proposed method was evaluated by simulation and experiment. In the proposed method, the controller is the integrator only, and it is a method that can intuitively tune the control performance by using the remaining two parameters. Because tuning can be done very easily, it is expected to be used in the industry.

The proposed method can be applied not only to joints of robots, however also to other applications that can be modeled into two-inertial systems.

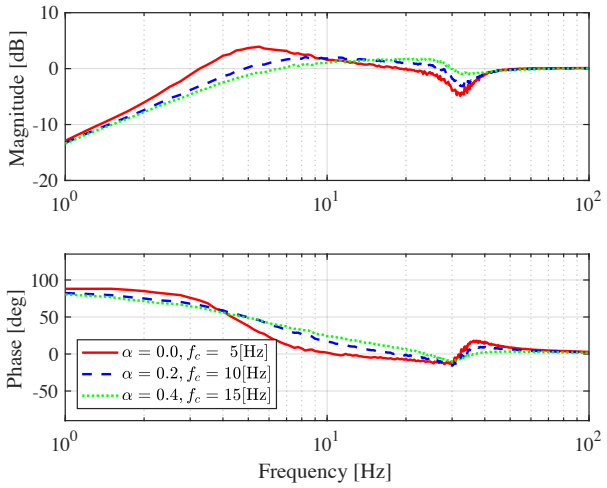

Fig. 16. Comparison of frequency characteristics of $\frac{\theta_L^{ref} - \theta_L}{\theta_L^{ref}}$ (Experiment)

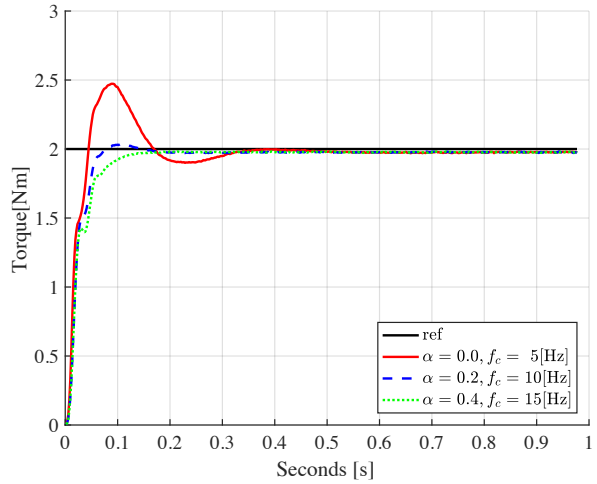

Fig. 17. Step response of T_S (Experiment)

References

(1) Koichi Sakata, Kazuaki Saiki, and Hiroshi Fujimoto. Self Resonance Cancellation using Multiple Sensors for Ballscrew Driven Stage. In *2011I EE-Japan Industry Application Society Conference (IEEJ JIASC 2011)*, No. 1, pp. 521–526, 2011.

(2) Yaskawa. Development of human-coexistent robot MOTOMAN-HC10 - Pioneering a new era of production equipment -(in Japanese). `https://www.yaskawa.co.jp/newsrelease/technology/13905`.

(3) TOYOTA. Partner Robot Family (Human Support Robot). `http://www.toyota-global.com/innovation/partner_robot/family_2.html`.

(4) Emre Sariyildiz and Kouhei Ohnishi. An Adaptive Reaction Force Observer Design. *IEEE/ASME Transactions on MechatronicsTRONICS*, Vol. 20, No. 2, pp. 750–760, 2015.

(5) Taro Takahashi, Yoshihiro Kuroki, Yusuke Kosaka, Eiji Niwa, Hiroshi Kaminaga, and Yoshihiko Nakamura. Development of flexible joint technology for human-coexisting robot on Cr-N thin film type torque sensor(in Japanese). *Toyota technical review*, pp. 128–134, 2015.

(6) UNIPULSE. Product information rotational torque meter (in japanese). `http://www.unipulse.com/jp/products/category_1_10.html`.

(7) Johan Pitelon, Rik Schoukens. *System Identification: A Frequency Domain Approach, 2nd Editon*. Wiley-IEEE Press, 2012.

(8) Koichi Sakata, Hiroyoshi Asaumi, Kazuyuki Hirachi, Kazuaki Saiki, and Hiroshi Fujimoto. Self Resonance Cancellation Techniques for a Two-Mass System and Its Application to a Large-Scale Stage. *IEEJ Journal of Industry Applications*, Vol. 3, No. 6, pp. 455–462, 2014.